Sectoral Differences in the Association of Optic Nerve Head Blood Flow and Glaucomatous Visual Field Defect Severity and Progression

Naoki Kiyota,[1] Yukihiro Shiga,[1,2] Masayuki Yasuda,[1] Naoko Aizawa,[1] Kazuko Omodaka,[1,2] Satoru Tsuda,[1] Hiroshi Kunikata,[1,3] and Toru Nakazawa[1–4]

[1]Department of Ophthalmology, Tohoku University Graduate School of Medicine, Miyagi, Japan
[2]Department of Ophthalmic Imaging and Information Analytics, Tohoku University Graduate School of Medicine, Miyagi, Japan
[3]Department of Retinal Disease Control, Tohoku University Graduate School of Medicine, Miyagi, Japan
[4]Department of Advanced Ophthalmic Medicine, Tohoku University Graduate School of Medicine, Miyagi, Japan

Correspondence: Toru Nakazawa, Department of Ophthalmology, Tohoku University Graduate School of Medicine, Sendai, Japan, 1-1 Seiryo-machi, Aoba-ku, Sendai 980-8574, Japan;
ntoru@oph.med.tohoku.ac.jp.

Submitted: April 2, 2019
Accepted: May 27, 2019

Citation: Kiyota N, Shiga Y, Yasuda M, et al. Sectoral differences in the association of optic nerve head blood flow and glaucomatous visual field defect severity and progression. *Invest Ophthalmol Vis Sci*. 2019;60:2650–2658. https://doi.org/10.1167/iovs.19-27230

Purpose. To investigate sectoral differences in the relationship between optic nerve head tissue blood flow, anatomically corresponding visual field defect severity, and future progression.

Methods. This retrospective longitudinal medical chart review comprised 508 eyes of 319 open-angle glaucoma patients (mean deviation: −9.2 ± 7.0 dB), followed for an average of 4.7 ± 1.1 years; an average 11.7 ± 3.7 visual field tests were performed. Average total deviation (TD) was calculated in the superior, central, and inferior sectors of the Humphrey 24-2 program. The optic nerve head was divided to obtain inferior, temporal, and superior tissue-area mean blur rate (MT), derived from laser speckle flowgraphy. At baseline, the correlation between MT and TD was compared in anatomically corresponding sectors. We performed a multivariate analysis to determine the contribution of baseline MT to corresponding TD slope and to determine background factors influencing superior to temporal MT. We used a linear-mixed effect model for the statistical analysis.

Results. At baseline, the highest β coefficients were found between MT-superior and TD-inferior, MT-temporal and TD-central, and between MT-inferior and TD-superior, in that order ($\beta = 0.38$, $\beta = 0.27$, $\beta = 0.26$, respectively). MT-superior and MT-temporal independently contributed to corresponding TD slope ($P < 0.05$). Male sex, high body mass index, and the prevalence of sleep apnea syndrome were contributing factors to lower superior to temporal MT ($P < 0.05$).

Conclusions. Review of medical history, measurements of systemic variables, and laser speckle flowgraphy parameters might help clinicians to predict visual field defect severity and progression.

Keywords: retinal blood flow, glaucoma, visual field

Although the only evidence-based and treatable risk factor for glaucoma is high intraocular pressure (IOP),[1] many glaucoma patients suffer from visual field (VF) defect progression even when their IOP is in the normal range. Thus, IOP-independent risk factors, such as vascular impairment, must be identified.[2–6] However, as local blood flow (BF) can also be reduced secondary to neurodegeneration,[7] it is difficult to determine the cause and effect relationship between these factors. Nevertheless, there have been various etiologic studies on the influence of blood pressure (BP) and ocular perfusion pressure (OPP) on the prevalence, incidence, and progression of glaucoma.[8] Unfortunately, these studies have disagreed, finding that both high and low BP and OPP were risk factors for glaucoma.[9–11] Meanwhile, several other studies have found no association.[12,13] These discrepancies might be because any kind of extreme change in BP, whether high or low, can cause BF reduction within the optic nerve head (ONH) (i.e., low diastolic BP causes low OPP and high systolic BP causes hypertensive vasoconstriction). To overcome this difficulty, direct ONH BF measurement might be preferred in this study field. Previous reports used laser Doppler flowmetry[14] or color Doppler imaging (CDI)[15–17] and reported that lower intraocular or retrobulbar BF at baseline was a risk factor for future glaucoma progression. Although these reports are valuable, they have several limitations specific to conventional BF measuring devices, such as their slow measurement time, low reproducibility, limited ability to measure BF within the deep areas of the ONH (i.e., CDI: retrobulbar, laser Doppler flowmetry: superficial ONH),[18–20] and inability to be used in a sectoral analysis.

Recently, laser speckle flowgraphy (LSFG) has been introduced as a clinical instrument for measuring ocular BF. LSFG is a quick, reproducible way to evaluate ocular BF.[21–27] The main parameter of LSFG is tissue-area mean blur rate (MT), which has been reported to represent BF in the deep regions of the ONH near the lamina cribrosa and has been found to be usable for interindividual comparisons.[21,28,29] In addition to these advantages, the LSFG software provides pulse waveform

parameters that have been reported to be associated with various systemic factors and ocular diseases.[23,30,31] Moreover, the software accompanying LSFG divides the ONH into four sectors, thus providing ONH-tissue BF parameters in different ONH sectors. It is known that glaucoma typically develops as inferior ONH rim degeneration and corresponding superior VF defects.[32] However, on the other hand, several reports indicate that systemic vascular impairment might contribute to atypical VF defects, involving the central to inferior field.[32–36] Therefore, an investigation of sectoral differences in the relationship between ONH-tissue BF and glaucomatous VF defects is important, and we believe the ability of LSFG to measure sector-by-sector ONH BF is advantageous for such an investigation.

In this retrospective medical chart review, we investigated sectoral differences in the relationship between baseline ONH-tissue BF, represented by MT, and anatomically corresponding VF defect severity and future VF defect progression. Based on the results of this analysis, we then investigated background factors influencing superior to temporal ONH-tissue BF.

Subjects and Methods

Subjects

Written informed consent was obtained from all participants before their participation. The procedures in this study followed the tenets of the Declaration of Helsinki and were approved by the institutional review board of the Tohoku University Graduate School of Medicine.

We retrospectively reviewed the medical records of 508 eyes of 319 open-angle glaucoma (OAG) patients (384 with normal-tension glaucoma [75.6%], 73 with primary OAG [21.4%], and 15 with unclassified OAG [2.9%]). The initial diagnosis was made by a glaucoma specialist (TN) between August 2012 and July 2015, and follow-up was performed at Tohoku University Hospital, located in Miyagi, Japan. After initial OAG diagnosis, each patient underwent a review of medical history, and baseline data were obtained for body height, weight, visual acuity, and IOP, as well as the results of slit-lamp, gonioscopic, and dilated funduscopic examinations. All patients met the following inclusion criteria in at least one eye: (1) glaucomatous changes to the optic disc at baseline, with corresponding VF defects, matching the Anderson-Patella criteria; (2) availability of follow-up data for at least 2 years and from 5 reliable VF tests; (3) LSFG and optical coherence tomography (OCT) data were available from within 3 months of baseline VF testing; (4) there was a normal, open angle in a gonioscopic examination; (5) IOP of $\leq$21 mm Hg, with or without medication, at baseline; (6) decimal best-corrected visual acuity of $\geq$0.7; (7) axial length of $\leq$26.5 mm; and (8) no intraocular surgery was performed during the follow-up period. When both eyes of a patient were eligible, both eyes were included in the analysis.

Measurement of Clinical Variables

IOP was measured with Goldmann applanation tonometry, axial length was measured with the IOL Master (Carl Zeiss Meditec, Dublin, CA, USA), and the VF was measured with the SITA standard 24-2 program of the Humphrey Field Analyzer (HFA) (Carl Zeiss Meditec); only measurements with fixation errors <20%, false positives <33%, and false negatives <33% were used. Circumpapillary retinal nerve fiber layer thickness (cpRNFLT) was measured with spectral-domain OCT (3D OCT-2000; Topcon, Inc., Tokyo, Japan). The accompanying software was used to divide the peripapillary area into four sectors, namely, superior, temporal, inferior, and nasal, to obtain cpRNFLT in each sector. Before the LSFG measurements, the patients sat in a quiet room for 10 minutes, following which BP and pulse rate were measured. Mean BP and OPP were calculated as follows: mean BP = diastolic BP + 1/3 (systolic BP – diastolic BP); OPP = 2/3 mean BP − IOP. When these measurements were performed more than once during the follow-up, the value measured at the closest date to baseline VF testing was selected for the analysis.

Assessment of Deep ONH BF With LSFG

ONH BF was assessed with the LSFG-NAVI device (Softcare Co., Ltd., Fukutsu, Japan), which measures mean blur rate (MBR) in arbitrary units (AUs). First, an ellipsoid was manually drawn around the ONH to define the region of interest in composite MBR color maps. The accompanying LSFG software (LSFG analyzer, version 3.1.59.0) then automatically divided the large-vessel and tissue (i.e., capillary) areas of the ONH and determined vessel-area MBR and tissue-area MBR (MT) separately.[37] The focus of this study was on MT, because it has been reported to be a good indicator of BF in the deep ONH (i.e., the area of the lamina cribrosa).[21,29] Furthermore, as all captured MBR images are synchronized to each cardiac cycle, LSFG can be used to calculate many pulse waveform parameters, including skew, blow-out score (BOS), blow-out time (BOT), rising rate (RR), falling rate (FR), flow acceleration index (FAI), acceleration time index (ATI), and resistivity index (RI). Schematic explanations and the formulas used to calculate these variables are described in detail elsewhere.[30,38] MBR and other waveform parameters were obtained in the overall ONH and in the superior, temporal, inferior, and nasal quadrants (Fig. 1).

Spatial Correspondence Among HVF Testing, OCT, and LSFG in This Study

The site-specific VF was evaluated in reference to the VF sector map established by Garway-Heath et al.[39] This study focused on the superior, central, and inferior VF sectors, (Fig. 1: red, orange and blue areas, respectively) because the VF sector corresponding to the nasal ONH is less important in glaucoma (Fig. 1: gray area).[40] Average total deviation (TD) and TD slope were calculated in each sector. The anatomic correspondence between HFA testing-derived TD and TD slope, OCT-derived cpRNFLT, and LSFG-derived MT is shown in Figure 1.

Statistical Analysis

All data are shown as the mean ± standard deviation. Univariate or multivariate linear mixed-effect models were used in this study. When we examined the data by sector, we set the subject variable as a random intercept. In other analyses, the "eye" variable was nested within the subject variable, which was set as a random intercept. The relationship between TD and LSFG-derived parameters in each sector was analyzed, adjusting for age because LSFG-derived parameters are related to age.[41] We then compared the slope between MT and TD with a multivariate model, setting MT as the response variable, and TD, age, the sectoral variable (temporal sector [reference, superior] or inferior sector [reference, superior]), and the interaction term between TD and the sectoral variable as explanatory variables. A multivariate model was used to determine contributing factors to TD slope in each sector. We then collected superior to temporal ONH data (i.e., inferior to central VF data) from each eye and used a univariate model to assess the effect of clinical factors on superior to temporal MT at baseline, adjusting for each sectoral variable (temporal

Investigative Ophthalmology & Visual Science

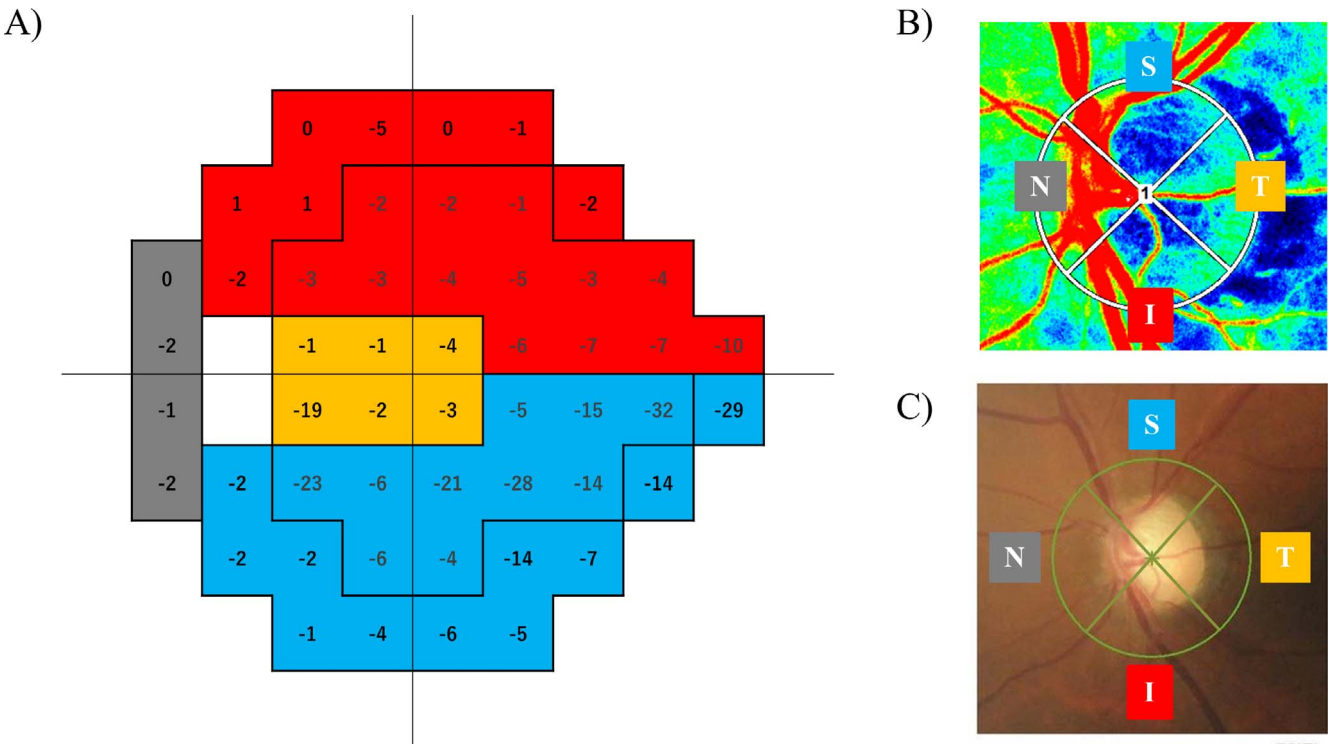

Figure 1. Representative diagram of VF sectors measured with the HFA 24-2 Swedish interactive threshold algorithm (**A**). LSFG color-map image (**B**) and OCT image (**C**). The site-specific VF was evaluated with the VF sectoral map established by Garway-Heath et al.[39] LSFG and OCT data for the nasal area, and the corresponding VF data, were excluded from the analysis (*gray color area*). The superior, temporal, and inferior LSFG and OCT-derived variables corresponded to the inferior, central, and superior HFA-derived variables in this study. The anatomic correspondence of this data is shown by matching colors (*red*, *orange*, and *blue*).

sector [reference, superior]) and the interaction term with the sectoral variable. The factors that reached statistical significance in this univariate analysis were retested in a multivariate analysis. All statistical analyses were performed with R software[42] (version 3.2.5). The significance level was set at $P < 0.05$.

Results

OCT and LSFG measurements were performed on the same date as baseline VF testing in 82.4% and 81.2% of cases, respectively. Patients were then followed for an average of 4.7 ± 1.1 years and an average of 11.7 ± 3.7 reliable VF tests were obtained. Table 1 shows the systemic characteristics and Table 2 shows the ocular characteristics of the patients, split by sex.

Table 1. Systemic Characteristics of OAG Patients

Characteristic	Male	Female
Number of patients	149	170
Age, y	62.0 ± 10.6	60.5 ± 11.8
BMI, kg/m^2	23.7 ± 3.0	22.1 ± 3.0
Systolic BP, mm Hg	127.7 ± 19.6	125.3 ± 18.4
Diastolic BP, mm Hg	78.5 ± 14.3	74.5 ± 13.7
Pulse rate, bpm	71.8 ± 13.1	76.2 ± 12.2
Smoking history, *n* (%)	24 (16.1)	4 (2.4)
Hypertensive medication, *n* (%)	57 (38.3)	49 (28.8)
Diabetes mellitus, *n* (%)	24 (16.1)	12 (7.1)
Dyslipidemia, *n* (%)	31 (20.8)	35 (20.6)
Heart disease, *n* (%)	23 (15.4)	20 (11.8)
SAS, *n* (%)	12 (8.1)	2 (1.2)
Migraine, *n* (%)	10 (6.7)	26 (15.3)

All data are shown as mean ± standard deviation.

Table 3 shows the relationship between LSFG-derived parameters and TD in each sector, after adjusting for age. TD-superior was statistically significantly correlated with MT-inferior, skew-inferior, BOS-inferior, BOT-inferior, FAI-inferior, and RI-inferior ($\beta = -0.18$ to 0.26, $P < 0.05$). TD-central was correlated with MT-temporal, skew-temporal, BOS-temporal, RR-temporal, FAI-temporal, and RI-temporal ($\beta = -0.25$ to 0.29, $P < 0.05$). TD-inferior was correlated with MT-superior, skew-superior, BOS-superior, BOT-superior, FR-superior, FAI-superior, ATI-superior, and RI-superior ($\beta = -0.32$ to 0.38, $P < 0.05$). As shown in Supplementary Table S1, a 1 dB increase in TD in a sector was associated with an increase in MT in the corresponding sector: 0.08 AU for MT-superior, 0.04 AU for MT-temporal, and 0.05 for MT-inferior. The slope between MT and TD was statistically higher between MT-superior and TD-inferior than between other sectors ($P < 0.001$). As shown in Table 4, contributions were made by baseline TD-superior and cpRNFLT-inferior to TD-superior slope ($\beta = -0.32$, $P < 0.001$; $\beta = 0.36$, $P < 0.001$, respectively), by baseline TD-central, cpRNFLT-temporal and MT-temporal to TD-central slope ($\beta = -0.10$, $P = 0.032$; $\beta = 0.11$, $P < 0.001$; $\beta = 0.20$, $P = 0.035$), and by TD-inferior, cpRNFLT-superior, and MT-superior to TD-inferior slope ($\beta = -0.29$, $P < 0.001$; $\beta = 0.28$, $P < 0.001$; $\beta = 0.17$, $P < 0.001$, respectively). Figure 2 shows scatterplots comparing MT and anatomically corresponding TD or TD slope.

Table 5 shows that lower cpRNFLT, older age, male sex, higher body mass index (BMI), the presence of diabetes mellitus, and the presence of sleep apnea syndrome (SAS) were associated with lower superior to temporal MT in the univariate analysis ($P < 0.05$). Male sex, higher BMI, and the presence of SAS remained significant in the multivariate

Table 2. Ocular Characteristics of OAG Patients

Characteristic	Male	Female
Number of eyes	227	281
IOP, mm Hg	13.0 ± 3.1	13.0 ± 2.7
Central corneal thickness, μm	516.5 ± 40.3	509 ± 35.6
Axial length, mm	24.7 ± 1.1	24.6 ± 1.3
Mean deviation, dB	−9.7 ± 7.4	−8.8 ± 6.6
TD-superior, dB	−10.9 ± 10.2	−10.4 ± 9.6
TD-central, dB	−7.0 ± 7.2	−7.3 ± 7.4
TD-inferior, dB	−9.7 ± 9.8	−8.1 ± 8.4
TD-nasal, dB	−3.0 ± 5.5	−3.3 ± 5.8
TD slope-superior, dB	−0.6 ± 1.0	−0.5 ± 0.9
TD slope-central, dB	−0.5 ± 1.0	−0.4 ± 0.9
TD slope-inferior, dB	−0.5 ± 1.0	−0.5 ± 0.9
TD slope-nasal, dB	−0.4 ± 0.9	−0.2 ± 0.8
CpRNFLT-overall, μm	80.7 ± 14.3	84.4 ± 13.4
CpRNFLT-superior, μm	94.4 ± 20.4	98.0 ± 22.4
CpRNFLT-temporal, μm	67.3 ± 16.4	74.8 ± 17.5
CpRNFLT-inferior, μm	86.3 ± 24.1	89.4 ± 21.1
CpRNFLT-nasal, μm	74.8 ± 15.6	75.2 ± 15.0
MT-overall, AU	9.2 ± 2.3	10.3 ± 2.3
MT-superior, AU	9.5 ± 2.9	10.9 ± 3.0
MT-temporal, AU	7.7 ± 2.3	8.4 ± 2.2
MT-inferior, AU	9.4 ± 2.5	10.6 ± 2.7
MT-nasal, AU	11.6 ± 2.8	12.7 ± 2.9
Prostaglandin analogues, *n* (%)	220 (96.9)	253 (90.0)
Beta-antagonists, *n* (%)	140 (61.7)	150 (53.4)
Carbonic anhydrase inhibitors, *n* (%)	153 (67.4)	149 (53.0)
Alpha2-stimulators, *n* (%)	115 (50.7)	95 (33.8)
Rho-kinase inhibitors, *n* (%)	13 (5.7)	13 (4.6)
Oral acetazolamide, *n* (%)	12 (5.3)	18 (6.4)

All data are shown as mean ± standard deviation.

Table 3. The Relationship Between LSFG-Derived Parameters and TD in Each Sector

Variables	β	*P*
TD-superior		
MT-inferior	0.26	<0.001*
Skew-inferior	0.12	0.008*
BOS-inferior	−0.18	<0.001*
BOT-inferior	−0.11	0.024*
RR-inferior	−0.02	0.630
FR-inferior	0.03	0.488
FAI-inferior	0.22	<0.001*
ATI-inferior	−0.06	0.156
RI-inferior	0.19	<0.001*
TD-central		
MT-temporal	0.27	<0.001*
Skew-temporal	0.09	0.039*
BOS-temporal	−0.25	<0.001*
BOT-temporal	−0.10	0.050
RR-temporal	−0.13	0.003*
FR-temporal	0.04	0.440
FAI-temporal	0.29	<0.001*
ATI-temporal	−0.09	0.052
RI-temporal	0.26	<0.001*
TD-inferior		
MT-superior	0.38	<0.001*
Skew-superior	0.20	<0.001*
BOS-superior	−0.32	<0.001*
BOT-superior	−0.17	<0.001*
RR-superior	−0.02	0.580
FR-superior	0.13	0.007*
FAI-superior	0.34	<0.001*
ATI-superior	−0.11	0.009*
RI-superior	0.33	<0.001*

Age was adjusted in this analysis. β, standard partial regression coefficient; *, indicates statistical significance.

analysis ($P < 0.05$). Figure 3 shows a representative image from an OAG patient who had SAS, low MT-superior with a delayed waveform peak, and progressive inferior VF defects.

Discussion

This retrospective longitudinal medical chart review included 508 eyes of 319 OAG patients who underwent OCT and LSFG measurement at baseline and longitudinal VF testing after the baseline. We investigated sectoral differences in the relationship between ONH-tissue BF and the severity of anatomically corresponding VF defects and future progression. We found that superior to temporal ONH-tissue BF was associated with both VF defect severity and future progression. Moreover, lower superior to temporal ONH-tissue BF was associated with SAS and factors associated with SAS, such as male sex and high BMI in a multivariate analysis. These results indicate that reviewing the medical history of patients and measuring systemic and LSFG variables might be valuable tools in predicting OAG severity and future VF defect progression.

We showed that superior ONH-tissue BF and corresponding inferior VF defect severity are more closely related than in other sectors in eyes with OAG. It has been reported that the inferior VF is more likely to be affected in glaucoma patients with diabetes mellitus.[43,44] Another study reported that normal-tension glaucoma patients with signs indicating ischemic changes in brain magnetic resonance imaging had a relatively deeper depression in the inferior pericentral VF area.[33] Additionally, nonarteritic anterior ischemic optic neuropathy (NA-AION) is known to typically develop into absolute inferionasal or inferior altitudinal VF defects.[45,46] These past reports, combined with our results, indicate that the superior ONH and corresponding inferior VF is vulnerable to hypoperfusion. The underlying mechanism is still unclear, although the anatomic location of the watershed zone might explain this pathophysiology. The watershed zone is the border between the territories fed by the short posterior ciliary arteries (SPCAs). It is an area of comparatively poor vascularity and, thus, is especially vulnerable to hypoperfusion.[47–49] It has been reported that approximately 60% of the watershed zone passes through the temporal half of the ONH, which links the medial and lateral SPCAs that encircle the posterior ONH.[50] Moreover, the common involvement of the inferior VF in NA-AION can be explained by the upper anastomosis appearing less proficient than the lower one.[46,49] We speculate that some subtypes of glaucoma might share this pathophysiology with NA-AION.

Additionally, it is interesting that not only low MT-superior but also low skew-superior, FAI-superior, FR-superior, RI-superior, high BOS-superior, BOT-superior, and ATI-superior were associated with inferior VF defect severity. Low MBR, FAI, and RI and high BOS and BOT indicate a relative decrease in the maximum minus minimum values of a waveform, i.e., waveform flattening. Low FAI, skew and high ATI indicate slower acceleration in the rising part of the waveform, accompanied by a delay in the peak of the waveform. Low FR indicates a convex, upward-pointing shape in the declining part of the waveform, which might be related to both waveform flattening and peak delay. We previously reported that slower acceleration and peak delay in the ONH-tissue waveform occurred more often in mild normal-tension glaucoma patients than controls.[23] We speculated that this

Table 4. The Effect of MT on Corresponding TD Slope, Adjusting for Other Baseline Clinical Parameters

Variable			
Dependent	**Independent**	**β**	***P* Value**
TD-superior slope	TD-superior	−0.32	<0.001*
	CpRNFLT-inferior	0.36	<0.001*
	MT-inferior	0.04	0.411
	Age	−0.02	0.725
	Axial length	0.12	0.055
	Center corneal thickness	−0.04	0.424
	OPP	0.05	0.283
	Pulse rate	0.04	0.419
TD-central slope	TD-central	−0.10	0.032*
	CpRNFLT-temporal	0.11	<0.001*
	MT-temporal	0.20	0.035*
	Age	−0.04	0.462
	Axial length	0.06	0.266
	Center corneal thickness	0.04	0.384
	OPP	0.06	0.195
	Pulse rate	0.01	0.912
TD-inferior slope	TD-inferior	−0.29	<0.001*
	CpRNFLT-superior	0.28	<0.001*
	MT-superior	0.17	<0.001*
	Age	−0.10	0.084
	Axial length	0.04	0.538
	Center corneal thickness	0.08	0.146
	OPP	0.04	0.495
	Pulse rate	0.06	0.287

β, standard partial regression coefficient; *, indicates statistical significance.

Table 5. Linear Mixed Effects Model Assessing the Effect of Clinical Factors on Superior to Temporal MT at Baseline

	Univariate		Multivariate	
Variables	**β**	***P* Value**	**β**	***P* Value**
CpRNFLT	0.35	<0.001	0.32	<0.001*
Age	−0.17	<0.001	−0.06	0.171
Male (reference, female)	−0.23	<0.001	−0.16	0.001*
BMI	−0.17	<0.001	−0.10	0.023*
Axial length	0.04	0.371		
Center corneal thickness	0.04	0.366		
IOP	0.01	0.907		
Systolic BP	−0.09	0.057		
Diastolic BP	−0.09	0.053		
Pulse rate	0.07	0.147		
Smoking history	−0.02	0.660		
Hypertensive medication	−0.09	0.063		
Diabetes mellitus	−0.13	0.011	−0.01	0.871
Dyslipidemia	−0.01	0.891		
Heart disease	0.04	0.458		
SAS	−0.15	0.002	−0.09	0.042*
Migraine	0.05	0.282		

Each sectoral variable (temporal sector [reference, superior]) and the interaction term were adjusted in this analysis. β, standard partial regression coefficient; *, indicates statistical significance.

waveform change represented endothelial dysfunction in the ONH-tissue microvasculature, especially when considering past studies in the field of cardiology.[51–53] The same logic can be applied to the results of the current study, but further investigation is needed for confirmation.

The most important finding of this study was the result of the multivariate analysis showing that superior to temporal ONH-tissue BF at baseline independently contributed to corresponding VF defect progression. Several reports have studied the association between baseline ocular BF and later glaucoma progression.[15,16,54–56] The majority of these studies used CDI to assess BF velocity in the retrobulbar vessels, such as the ophthalmic artery, central retinal artery, and SPCA. Though SPCA is usually the main point of interest in this study field because the SPCA perfuses the lamina cribrosa, which is believed to be the primary site of lesion in glaucoma,[57] few

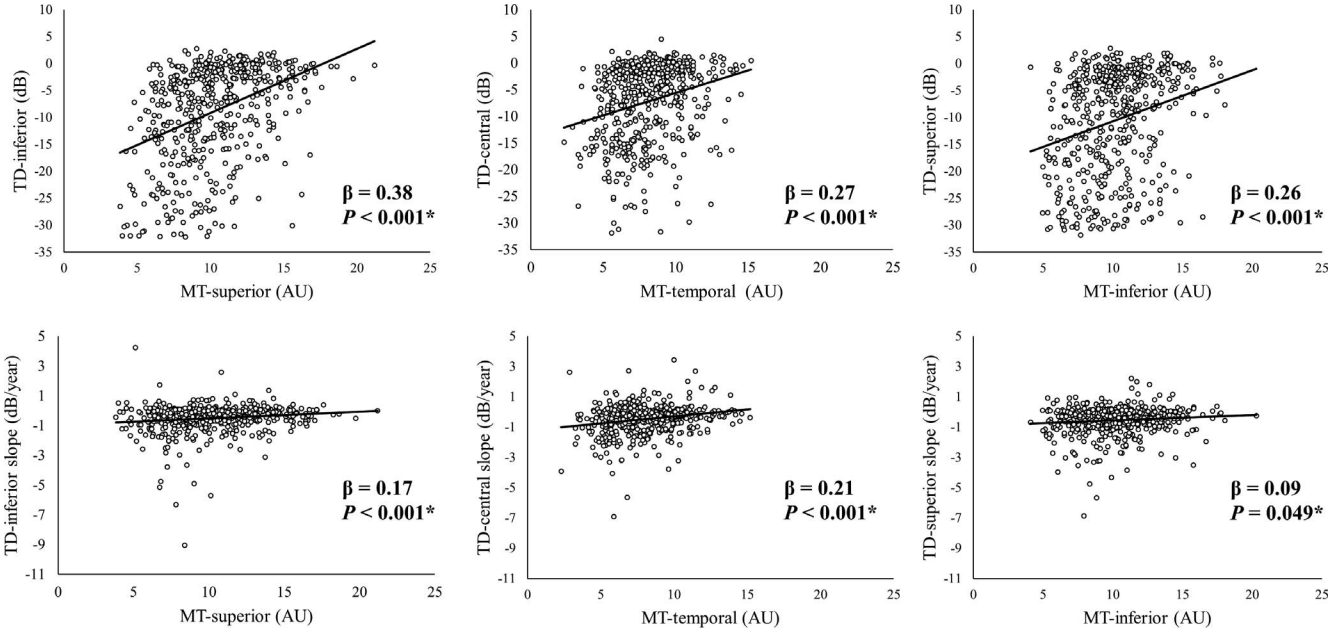

Figure 2. Scatterplots showing the relationship between MT and corresponding TD or TD slope in each sector. β indicates the standardized regression coefficient, adjusting for age. *Asterisks* indicate statistical significance. There were significant correlations between MT and TD (β = 0.26 − 0.38, $P < 0.001$), and between MT and TD slope (β = 0.09 − 0.17, $P < 0.05$).

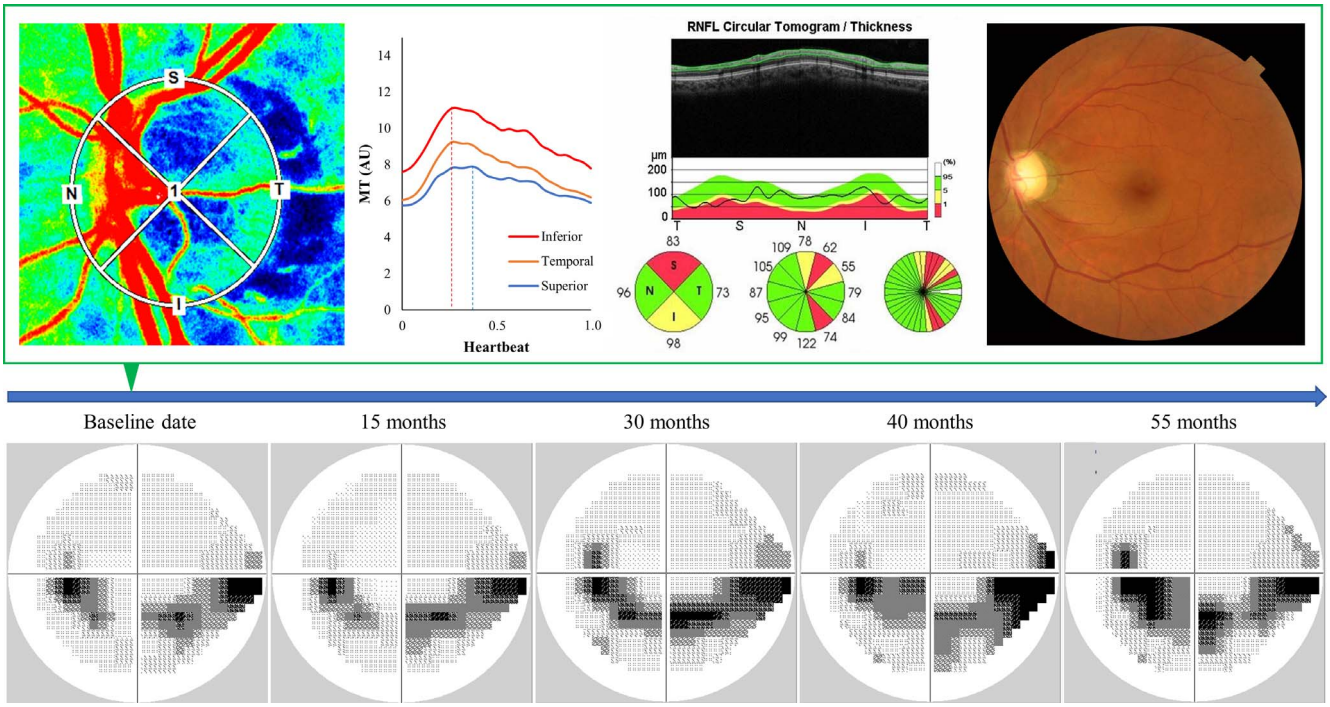

Figure 3. Data from a representative OAG eye with insufficient ONH-tissue BF. The *upper panel* shows an LSFG map, the waveform for inferior, temporal, and superior ONH-tissue BF, OCT data, and a baseline fundus photograph from left to right. The *lower panel* shows longitudinal changes in the gray-scale VF (HFA; 24-2 Swedish interactive threshold algorithm) until 55 months after baseline VF testing. The patient was a 55-year-old male with a history of SAS and hypertension. ONH-tissue BF in the superior sector shows a more flattened waveform, slower acceleration in a rising curve, and a more delayed peak (shown by the *dotted line*) than in other sectors. Other data for this patient were as follows: axial length, 24.9 mm; central corneal thickness, 501 μm; IOP, 10 mm Hg; BP, 112/69 mm Hg; pulse rate, 58 beats per minute (bpm); MD, −7.1 dB; TD-superior, −4.4 dB; TD-central, −5.0 dB; TD-inferior, −15.4 dB; MD slope, −1.0 dB/year; TD-superior slope, −1.2 dB/year; TD-central slope, −1.6 dB/year; TD-inferior slope, −1.7 dB/year; cpRNFLT-inferior, 98.4 μm; cpRNFLT-temporal, 73.0 μm; and cpRNFLT-superior, 82.9 μm.

studies have succeeded in showing an association between SPCA circulation and glaucoma progression.[16,54–56] This may be because the SPCAs are hard to detect due to their small size and measurements thus have lower reproducibility.[18,58] By contrast, measurements made with LSFG have the advantage of being able to directly evaluate SPCA-derived ONH-tissue BF, represented by MT, quickly and reproducibly.[19,26,59] Importantly, we also found that low BF was still a contributing factor to VF defect progression after matching for same-sector cpRNFLT values. Matching parameters related to ONH structure is important because BF reduction and glaucomatous neurodegeneration are considered to proceed in parallel, each contributing to the other.[7] The results of our multivariate linear mixed-effect model analysis support the theory that BF reduction can be a primary cause of later VF defect progression in the superior to temporal sector quadrants, although such a trend is not clear in the inferior sector. As discussed above, anatomic features of the superior and temporal sectors make these regions vulnerable to hypoperfusion and might thus explain these findings. However, a definitive explanation of these results awaits a future study with a larger sample size and longer follow-up period.

Several background factors may have influenced our finding that superior to temporal ONH-tissue BF was associated with both corresponding VFD severity and future VFD progression. We found that SAS, male sex, and high BMI were significantly associated with lower superior to temporal ONH-tissue BF, even after adjustment for same-sector cpRNFLT values and other confounding factors. Interestingly, these factors have been reported to be associated with each other and can be linked to SAS.[60–62] There have been many reports indicating an association between SAS and the pathophysiology of glaucoma.[63,64] Early reports on this association speculated that it was caused by increased IOP during apnea events while sleeping, but later, it was demonstrated that apnea events in fact significantly reduced average IOP.[65] Therefore, IOP-independent factors, including vascular impairment, have become increasingly suspected as explaining the close link between SAS and glaucoma. In comparison to females, males with obesity typically show increased upper-body fat, including in the neck, where it can lead to airway obstruction.[66] As a reaction to life-threatening airway obstruction, hypoxemia and sympathetic nerve activation can occur, leading to vascular endothelial dysfunction.[67] We speculate that OAG patients with SAS develop atherosclerotic changes in the ocular vessels and that this then leads to ONH-tissue BF impairment. However, a prospective study will be necessary to clarify the mechanism underlying our findings.

Our study has several limitations. First, it was a retrospective, longitudinal study of patients of a single ethnicity, and the patients were followed for varying lengths of time with a varying number of VF tests. Therefore, there is a need for a future prospective, longitudinal study with a more diverse population to confirm our results. Second, the current study emphasized baseline predictors of progression. Changes over time in cpRNFLT, MT, and other factors were not assessed during the follow-up. Further investigation of these factors and relationships may help to better understand glaucoma progression. Third, our observation of a stronger correlation between MT-superior and TD-inferior and TD-inferior slope might simply be due to a more limited distribution of values, with the values for opposite-side TD-superior having a narrower range. Although the average value was worse for TD-superior than TD-inferior, reflecting the characteristics of

glaucomatous VF defects, both ranged widely (TD-inferior: from −33.8 to 2.5 dB; TD-superior: from −32.8 to 2.5 dB). Additionally, when we added TD-superior to the third model, shown in Table 4, the contribution of MT-superior was almost unchanged ($\beta = 0.17$, $P < 0.001$) and model fitting did not improve ($P = 0.890$, ANOVA), indicating that the contribution of MT-superior to TD-inferior slope was not affected by the severity of opposite-side TD-superior. A possible fourth limitation of our study was the use of medication by our subjects. Several types of antiglaucoma eye drops have been reported to have a protective effect on BF.[68–71] However, considering that patients with more severe glaucoma take more antiglaucoma medications, VF defect severity and its progression would likely have been even worse without the use of these drugs. Therefore, it is unlikely that these drugs led to an overestimation of the association between ONH-tissue BF and corresponding VF defect severity and progression. Fifth, as our review of the patients' medical history was based on self-reporting, we might have over- or underestimated the prevalence of systemic diseases. However, we believe that our finding of prevalence of SAS is reasonable because it matches the other observed variables, which have reported to be associated with SAS. Nevertheless, a future investigation including a detailed, objective assessment of SAS, such as provided by apnea hypopnea index, is needed.

In conclusion, this retrospective medical chart review revealed that superior to temporal ONH-tissue BF might be affected by SAS and was related to anatomically corresponding VF defect severity and future VF defect progression. These results indicate that medical history review, measurement of systemic variables, and measurement with LSFG might be useful in glaucoma care.

Acknowledgments

Supported in part by the JSPS KAKENHI Grants-in-Aid for Scientific Research (B) (TN; 26293372), for Exploratory Research (TN; 26670751), and by JST Center for Revitalization Promotion.

Disclosure: **N. Kiyota**, None; **Y. Shiga**, None; **M. Yasuda**, None; **N. Aizawa**, None; **K. Omodaka**, None; **S. Tsuda**, None; **H. Kunikata**, None; **T. Nakazawa**, None

References

1. The AGIS Investigators. The Advanced Glaucoma Intervention Study (AGIS): 7. The relationship between control of intraocular pressure and visual field deterioration. *Am J Ophthalmol*. 2000;130:429–440.
2. Nakazawa T. Ocular blood flow and influencing factors for glaucoma. *Asia-Pacific J Ophthalmol (Phila)*. 2016;5:38–44.
3. Kiyota N, Kunikata H, Takahashi S, Shiga Y, Omodaka K, Nakazawa T. Factors associated with deep circulation in the peripapillary chorioretinal atrophy zone in normal-tension glaucoma with myopic disc. *Acta Ophthalmol*. 2018;96:e290–e297.
4. Shiga Y, Aizawa N, Tsuda S, et al. Preperimetric Glaucoma Prospective Study (PPGPS): predicting visual field progression with basal optic nerve head blood flow in normotensive PPG eyes. *Trans Vis Sci Tech*. 2018;7(1):11.
5. Fan N, Wang P, Tang L, Liu X. Ocular blood flow and normal tension glaucoma. *Biomed Res Int*. 2015;2015:1–7.
6. Lee NY, Jung Y, Han K, Park CK. Fluctuation in systolic blood pressure is a major systemic risk factor for development of primary open-angle glaucoma. *Sci Rep*. 2017;7:43734.
7. Cull G, Told R, Burgoyne CF, Thompson S, Fortune B, Wang L. Compromised optic nerve blood flow and autoregulation secondary to neural degeneration. *Invest Ophthalmol Vis Sci*. 2015;56:7286–7292.
8. Costa VP, Harris A, Anderson D, et al. Ocular perfusion pressure in glaucoma. *Acta Ophthalmol*. 2014;92:e252–e266.
9. Tielsch JM, Katz J, Sommer A, Quigley HA, Javitt JC. Hypertension, perfusion pressure, and primary open-angle glaucoma. A population-based assessment. *Arch Ophthalmol*. 1995;113:216–221.
10. Bonomi L, Marchini G, Marraffa M, Bernardi P, Morbio R, Varotto A. Vascular risk factors for primary open angle glaucoma: the Egna-Neumarkt Study. *Ophthalmology*. 2000;107:1287–1293.
11. Memarzadeh F, Ying-Lai M, Chung J, Azen SP, Varma R; Los Angeles Latino Eye Study Group. Blood pressure, perfusion pressure, and open-angle glaucoma: the Los Angeles Latino Eye Study. *Invest Ophthalmol Vis Sci*. 2010;51:2872–2877.
12. Jonas JB, Xu L, Wang YX. The Beijing eye study. *Acta Ophthalmol*. 2009;87:247–261.
13. Ramdas WD, Wolfs RCW, Hofman A, de Jong PTVM, Vingerling JR, Jansonius NM. Lifestyle and risk of developing open-angle glaucoma: the Rotterdam study. *Arch Ophthalmol*. 2011;129:767–772.
14. Zink JM, Grunwald JE, Piltz-Seymour J, Staii A, Dupont J. Association between lower optic nerve laser Doppler blood volume measurements and glaucomatous visual field progression. *Br J Ophthalmol*. 2003;87:1487–1491.
15. Magureanu M, Stanila A, Bunescu LV, Armeanu C. Color Doppler imaging of the retrobulbar circulation in progressive glaucoma optic neuropathy. *Rom J Ophthalmol*. 2016;60:237–248.
16. Yamazaki Y, Drance SM. The relationship between progression of visual field defects and retrobulbar circulation in patients with glaucoma. *Am J Ophthalmol*. 1997;124:287–295.
17. Zeitz O, Galambos P, Wagenfeld L, et al. Glaucoma progression is associated with decreased blood flow velocities in the short posterior ciliary artery. *Br J Ophthalmol*. 2006;90:1245–1248.
18. Galassi F, Sodi A, Ucci F, Renieri G, Pieri B, Baccini M. Ocular hemodynamics and glaucoma prognosis: a color Doppler imaging study. *Arch Ophthalmol*. 2003;121:1711–1715.
19. Sugiyama T, Araie M, Riva CE, Schmetterer L, Orgul S. Use of laser speckle flowgraphy in ocular blood flow research. *Acta Ophthalmol*. 2010;88:723–729.
20. Langhans M, Michelson G, Groh MJM. Effect of breathing 100% oxygen on retinal and optic nerve head capillary blood flow in smokers and non-smokers. *Br J Ophthalmol*. 1997;81:365–369.
21. Wang L, Cull GA, Piper C, Burgoyne CF, Fortune B. Anterior and posterior optic nerve head blood flow in nonhuman primate experimental glaucoma model measured by laser speckle imaging technique and microsphere method. *Invest Ophthalmol Vis Sci*. 2012;53:8303–8309.
22. Kiyota N, Shiga Y, Takahashi H, Nakazawa T. Large vessel area of the optic nerve head, measured with laser speckle flowgraphy, is significantly reduced in eyes with preperimetric glaucoma. *Clin Experiment Ophthalmol*. 2015;43:841–843.
23. Shiga Y, Omodaka K, Kunikata H, et al. Waveform analysis of ocular blood flow and the early detection of normal tension glaucoma. *Invest Ophthalmol Vis Sci*. 2013;54:7699–7706.
24. Luft N, Wozniak PA, Aschinger GC, et al. Measurements of retinal perfusion using laser speckle flowgraphy and doppler optical coherence tomography. *Invest Ophthalmol Vis Sci*. 2016;57:5417–5425.
25. Luft N, Wozniak PA, Aschinger GC, et al. Ocular blood flow measurements in healthy white subjects using laser speckle flowgraphy. *PLoS One*. 2016;11:e0168190.
26. Kiyota N, Shiga Y, Suzuki S, et al. The effect of systemic hyperoxia on optic nerve head blood flow in primary open-

angle glaucoma patients. *Invest Ophthalmol Vis Sci*. 2017;58:3181–3188.

27. Kiyota N, Kunikata H, Shiga Y, Omodaka K, Nakazawa T. Relationship between laser speckle flowgraphy and optical coherence tomography angiography measurements of ocular microcirculation. *Graefes Arch Clin Exp Ophthalmol*. 2017;255:1633–1642.
28. Shiga Y, Shimura M, Asano T, et al. The influence of posture change on ocular blood flow in normal subjects, measured by laser speckle flowgraphy. *Curr Eye Res*. 2013;38:691–698.
29. Aizawa N, Nitta F, Kunikata H, et al. Laser speckle and hydrogen gas clearance measurements of optic nerve circulation in albino and pigmented rabbits with or without optic disc atrophy. *Invest Ophthalmol Vis Sci*. 2014;55:7991–7996.
30. Tsuda S, Kunikata H, Shimura M, et al. Pulse-waveform analysis of normal population using laser speckle flowgraphy. *Curr Eye Res*. 2014;39:1207–1215.
31. Yanagida K, Iwase T, Yamamoto K, et al. Sex-related differences in ocular blood flow of healthy subjects using laser speckle flowgraphy. *Invest Ophthalmol Vis Sci*. 2015;56:4880–4890.
32. Park H-YL, Jung K-I, Na K-S, Park S-H, Park C-K. Visual field characteristics in normal-tension glaucoma patients with autonomic dysfunction and abnormal peripheral microcirculation. *Am J Ophthalmol*. 2012;154:466–475.e1.
33. Suzuki J, Tomidokoro A, Araie M, et al. Visual field damage in normal-tension glaucoma patients with or without ischemic changes in cerebral magnetic resonance imaging. *Jpn J Ophthalmol*. 2004;48:340–344.
34. Sung KR, Cho JW, Lee S, et al. Characteristics of visual field progression in medically treated normal-tension glaucoma patients with unstable ocular perfusion pressure. *Invest Ophthalmol Vis Sci*. 2011;52:737–743.
35. Park SC, De Moraes CG, Teng CCW, Tello C, Liebmann JM, Ritch R. Initial parafoveal versus peripheral scotomas in glaucoma: risk factors and visual field characteristics. *Ophthalmology*. 2011;118:1782–1789.
36. Liu C, Su W, Shie S, Cheng S, Su C-W, Ho W-J. Association between peripheral vascular endothelial function and progression of open-angle glaucoma. *Medicine (Baltimore)*. 2016;95:e3055.
37. Chiba N, Omodaka K, Yokoyama Y, et al. Association between optic nerve blood flow and objective examinations in glaucoma patients with generalized enlargement disc type. *Clin Ophthalmol*. 2011;5:1549–1556.
38. Sugiyama T. Basic technology and clinical applications of the updated model of laser speckle flowgraphy to ocular diseases. *Photonics*. 2014;1:220–234.
39. Garway-Heath DF, Poinoosawmy D, Fitzke FW, Hitchings RA. Mapping the visual field to the optic disc in normal tension glaucoma eyes. *Ophthalmology*. 2000;107:1809–1815.
40. Jonas JB, Budde WM. Is the nasal optic disc sector important for morphometric glaucoma diagnosis? *Br J Ophthalmol*. 2002;86:1232–1235.
41. Luft N, Wozniak PA, Aschinger GC, et al. Ocular blood flow measurements in healthy white subjects using laser speckle flowgraphy. *PLoS One*. 2016;11:e0168190.
42. R Core Team. A language and environment for statistical computing. R Foundation for Statistical Computing, Vienna, Austria. Available at: https://www.R-project.org/.
43. Zeiter JH, Shin DH, Baek NH. Visual field defects in diabetic patients with primary open-angle glaucoma. *Am J Ophthalmol*. 1991;111:581–584.
44. Zeiter JH, Shin DH. Diabetes in primary open-angle glaucoma patients with inferior visual field defects. *Graefes Arch Clin Exp Ophthalmol*. 1994;232:205–210.
45. Hayreh SS, Zimmerman B. Visual field abnormalities in nonarteritic anterior ischemic optic neuropathy: their pattern and prevalence at initial examination. *Arch Ophthalmol*. 2005;123:1554–1562.
46. Kerr NM, Chew SSSL, Danesh-Meyer HV. Non-arteritic anterior ischaemic optic neuropathy: a review and update. *J Clin Neurosci*. 2009;16:994–1000.
47. Hayreh SS. The blood supply of the optic nerve head and the evaluation of it—myth and reality. *Prog Retin Eye Res*. 2001;20:563–593.
48. Hayreh SS. Posterior ciliary artery circulation in health and disease: the Weisenfeld lecture. *Invest Ophthalmol Vis Sci*. 2004;45:749–757.
49. Olver JM, Spalton DJ, McCartney AC. Microvascular study of the retrolaminar optic nerve in man: the possible significance in anterior ischaemic optic neuropathy. *Eye (Lond)*. 1990;4:7–24.
50. Hayreh SS. In vivo choroidal circulation and its watershed zones. *Eye (Lond)*. 1990;4:273–289.
51. White CR, Haidekker M, Bao X, Frangos JA. Temporal gradients in shear, but not spatial gradients, stimulate endothelial cell proliferation. *Circulation*. 2001;103:2508–2513.
52. Hsiai TK, Cho SK, Honda HM, et al. Endothelial cell dynamics under pulsating flows: significance of high versus low shear stress slew rates (d(tau)/dt). *Ann Biomed Eng*. 2002;30:646–656.
53. Davies PF, Dewey CF, Bussolari SR, Gordon EJ, Gimbrone MA. Influence of hemodynamic forces on vascular endothelial function. In vitro studies of shear stress and pinocytosis in bovine aortic cells. *J Clin Invest*. 1984;73:1121–1129.
54. Zeitz O, Galambos P, Wagenfeld L, et al. Glaucoma progression is associated with decreased blood flow velocities in the short posterior ciliary artery. *Br J Ophthalmol*. 2006;90:1245–1248.
55. Satilmis M, Orgül S, Doubler B, Flammer J. Rate of progression of glaucoma correlates with retrobulbar circulation and intraocular pressure. *Am J Ophthalmol*. 2003;135:664–669.
56. Martínez A, Sánchez M. Predictive value of colour Doppler imaging in a prospective study of visual field progression in primary open-angle glaucoma. *Acta Ophthalmol Scand*. 2005;83:716–722.
57. Anderson DR. Ultrastructure of human and monkey lamina cribrosa and optic nerve head. *Arch Ophthalmol*. 1969;82:800–814.
58. Xu G, Weinreb RN, Leung CKS. Optic nerve head deformation in glaucoma: the temporal relationship between optic nerve head surface depression and retinal nerve fiber layer thinning. *Ophthalmology*. 2014;121:2362–2370.
59. Aizawa N, Yokoyama Y, Chiba N, et al. Reproducibility of retinal circulation measurements obtained using laser speckle flowgraphy-NAVI in patients with glaucoma. *Clin Ophthalmol*. 2011;5:1171–1176.
60. Bixler EO, Vgontzas AN, Lin HM, et al. Prevalence of sleep-disordered breathing in women: effects of gender. *Am J Respir Crit Care Med*. 2001;163:608–613.
61. Jehan S, Zizi F, Pandi-Perumal SR, et al. Obstructive sleep apnea and obesity: implications for public health. *Sleep Med Disord Int J*. 2017;1:1310–1314.
62. Romero-Corral A, Caples SM, Lopez-Jimenez F, Somers VK. Interactions between obesity and obstructive sleep apnea: implications for treatment. *Chest*. 2010;137:711–719.
63. Mojon DS, Hess CW, Goldblum D, et al. High prevalence of glaucoma in patients with sleep apnea syndrome. *Ophthalmology*. 1999;106:1009–1012.

Investigative Ophthalmology & Visual Science

64. Karakucuk S, Goktas S, Aksu M, et al. Ocular blood flow in patients with obstructive sleep apnea syndrome (OSAS). *Graefes Arch Clin Exp Ophthalmol*. 2008;246:129–134.

65. Shinmei Y, Nitta T, Saito H, et al. Continuous intraocular pressure monitoring during nocturnal sleep in patients with obstructive sleep apnea syndrome. *Invest Opthalmology Vis Sci*. 2016;57:2824–2830.

66. Kapsimalis F, Kryger MH. Gender and obstructive sleep apnea syndrome, part 1: clinical features. *Sleep*. 2002;25:412–419.

67. Kario K. Obstructive sleep apnea syndrome and hypertension: mechanism of the linkage and 24-h blood pressure control. *Hypertens Res*. 2009;32:537–541.

68. Sugiyama T, Azuma I. Effect of UF-021 on optic nerve head circulation in rabbits. *Jpn J Ophthalmol*. 1995;39:124–129.

69. Tsuda S, Yokoyama Y, Chiba N, et al. Effect of topical tafluprost on optic nerve head blood flow in patients with myopic disc type. *J Glaucoma*. 2013;22:398–403.

70. Fuchsjäger-Mayrl G, Wally B, Rainer G, et al. Effect of dorzolamide and timolol on ocular blood flow in patients with primary open angle glaucoma and ocular hypertension. *Br J Ophthalmol*. 2005;89:1293–1297.

71. Liu CJ-L, Ko Y-C, Cheng C-Y, Chou JC, Hsu W-M, Liu J-H. Effect of latanoprost 0.005% and brimonidine tartrate 0.2% on pulsatile ocular blood flow in normal tension glaucoma. *Br J Ophthalmol*. 2002;86:1236–1239.

Investigative Ophthalmology & Visual Science